HHS Public Access

Author manuscript

J Surg Res. Author manuscript; available in PMC 2017 November 01.

Published in final edited form as:

J Surg Res. 2016 November ; 206(1): 118–125. doi:10.1016/j.jss.2016.07.020.

Murine model of long term obstructive jaundice

Hiroaki Aoki, MD PhD[1,2], **Masayo Aoki, MD PhD**[1,2], **Jing Yang, BS**[3], **Eriko Katsuta, MD PhD**[1,2], **Partha Mukhopadhyay, PhD**[1,2], **Rajesh Ramanathan, MD**[1], **Ingrid A. Woelfel, BS**[1,2], **Xuan Wang**[3], **Sarah Spiegel, PhD**[2], **Huiping Zhou, PhD**[3], and **Kazuaki Takabe, MD, PhD, FACS**[1,2]

[1]Division of Surgical Oncology, Department of Surgery, Virginia Commonwealth University School of Medicine, West Hospital 7-402, 1200 East Broad Street, Richmond, Virginia 23298

[2]Department of Biochemistry and Molecular Biology, Virginia Commonwealth University School of Medicine, West Hospital 7-402, 1200 East Broad Street, Richmond, Virginia 23298

[3]Department of Microbiology and Immunology, Virginia Commonwealth University School of Medicine, West Hospital 7-402, 1200 East Broad Street, Richmond, Virginia 23298

[4]Breast Surgery, Roswell Park Cancer Institute, Buffalo NY 14263

Abstract

Background—With the recent emergence of conjugated bile acids as signaling molecules in cancer, a murine model of obstructive jaundice by cholestasis with long-term survival is in need. Here, we investigated the characteristics of 3 murine models of obstructive jaundice.

Methods—C57BL/6J mice were used for total ligation of the common bile duct (tCL), partial common bile duct ligation (pCL), and ligation of left and median hepatic bile duct with gallbladder removal (LMHL) models. Survival was assessed by Kaplan-Meier method. Fibrotic change was determined by Masson-Trichrome staining and Collagen expression.

Results—70% (7/10) of tCL mice died by Day 7, whereas majority 67% (10/15) of pCL mice survived with loss of jaundice. 19% (3/16) of LMHL mice died; however, jaundice continued beyond Day 14, with survival of more than a month. Compensatory enlargement of the right lobe was observed in both pCL and LMHL models. The pCL model demonstrated acute inflammation due to obstructive jaundice 3 days after ligation but jaundice rapidly decreased by Day 7. The LHML group developed portal hypertension as well as severe fibrosis by Day 14 in addition to prolonged jaundice.

Corresponding author: Kazuaki Takabe MD PhD FACS, Breast Surgery, Roswell Park Cancer Institute, Elm & Carlton Streets, Buffalo NY 14263 USA, Tel: 716-845-5128, Fax: (716) 845-5705, Kazuaki.takabe@roswellpark.org.

Author contributions:

HA performed experiments, and prepared the manuscript. MA and EK contributed to development of the model and provided feedback and instruction in methodology. PM, JY, XW, and HZ conducted the molecular biological and biochemical experiments. RR, SS and TK contributed in discussion and editing. KT conceptualized and prepared the manuscript.

Disclosure:

This manuscript was presented at the 11th Annual Academic Surgical Congress at Jacksonville, FL

Conclusion—The standard tCL model is too unstable with high mortality for long-term studies. pCL may be an appropriate model for acute inflammation with obstructive jaundice but long term survivors are no longer jaundiced. The LHML model was identified to be the most feasible model to study the effect of long-term obstructive jaundice.

1. Introduction

Obstructive jaundice is often one of the clinical signs of blockage of biliary tract. For instance, advanced cholangiocarcinoma, cancer of the bile duct, is commonly associated with obstructive jaundice after development of bile duct obstruction. Obstruction of the biliary tract results in elevated levels of primary and conjugated bile acids (CBAs), which have recently been shown to promote cholangiocarcinoma progression [1–3].

During the last decade, bile acids have been recognized not only as detergents, but also as important signaling molecules involved in the regulation of metabolism [4–6]. Recently, we found that CBAs activate the cell proliferation and survival signaling pathways primarily through binding to sphingosine-1-phosphate receptor 2 (S1PR2) in hepatocytes [5]. We further discovered that CBAs activate S1PR2 and upregulate expression of sphingosine kinase 2 in the nucleus of hepatocytes that epigenetically regulate lipid and sterol metabolism in the liver [6]. Thus, indicating that bile acid signaling via S1PR2 and SphK2 plays pivotal roles in the liver. Following our results, CBAs were also found to promote the growth and invasion of cholangiocarcinoma cells via activation of S1PR2 *in vitro* [2]. This is possibly due to induction of cyclooxygenase-2 expression [1].

One of the obstacles that hinder the progress of this field of research is the lack of an appropriate animal model of obstructive jaundice. The most commonly used standard murine model is the Total Common bile duct Ligation (tCL) model. There have been mixed reports on the survival of animals in this model, with survival rates ranging from around 10% perioperative mortality [7–10] to up to 60 days [11]. In general, however, this model is considered unstable with short survival. The Partial Common bile duct Ligation model (pCL) was established to improve survival so that the long term effect of obstructive jaundice can be studied [12]. Another model is the Left and Middle Hepatic duct Ligation model (LMHL). This model includes hepatic bile duct ligation distal to the merging point of the left and middle hepatic bile duct and proximal to the union of the right and caudate hepatic bile duct, in addition to gallbladder removal [3].

To date, there have been no reports to our knowledge that directly compare these models. Here, we investigated the characteristics of the most commonly used tCL model, and pCL and LMHL models to clarify their utility and identify which one will be the most feasible long term obstructive jaundice model.

2. Material and methods

2.1. Animals

All animal studies were conducted in the Animal Research Core Facility at Virginia Commonwealth University School of Medicine in accordance with institutional guidelines.

Surgical procedures were approved by the Virginia Commonwealth University Institutional Animal Care and Use Committee (IACUC), accredited by the Association for Assessment and Accreditation of Laboratory Animal Care. Male C57BL/6J (8–26 week, weight 20–35 g; The Jackson Laboratory, Bar Harbor, ME) were anesthetized with continuous vaporized 2% isoflurane for general anesthesia. The mice were given analgesia (Buprenorphine SR or Meloxicam SR, Zoopharm, Windsor, CO) for at least 72 hours postoperatively and closely monitored throughout the perioperative period. After the procedures the mice were kept on a warming pad in their cage warmed up by an infrared lamp until the mice were fully awake and active. Any animals appearing to be in significant distress or showing physical signs indicating unlikely survival for an additional 24 h were euthanized as a humane end point based upon our IACUC protocol. In order to achieve stable results, we found that 10 operations in each model were necessary to obtain the appropriate surgical expertise. Male mice were chosen following previous publications of obstructive jaundice models. The numbers of mice to be used for each cohort were chosen based upon the previous studies.

2.2 RNA Isolation and Quantitative Real-Time Reverse-Transcriptase Polymerase Chain Reaction

Total cellular RNA was isolated using Trizol reagent (QIA- GEN, Inc, Valencia, CA) and reverse transcribed into first-strand complementary DNA (cDNA) using the High-Capacity cDNA Reverse Transcription Kit from Life Technologies. Messenger RNA (mRNA) levels of collagen 1a1 were determined by real-time reverse-transcriptase polymerase chain reaction (RT- PCR) using iQTM SYBR Green Supermix reagents and normalized glyceraldehyde 3-phosphate dehydrogenase (GAPDH) as an internal control. Sequences of these primers were:

5’-GGC GGT TCA GGT CCA ATG-3’ (Collagen1a1 forward)

5’-GTT CCA GGCAAT CCA CGA-3’ (Collagen1a1 reverse)

5’ GTC GTG GAT CTG ACG TGC C-3’ (GAPDH forward)

5’-GAT GCC TGC TTC ACC ACC TT-3’ (GAPDH reverse)

2.3 Bile Acid measurement

Mouse Bile Acids Assay Kit (Crystal Chem, Zaandam, Netherlands) was used for measuring the serum concentration of total bile acids.

2.4 Histological analyses

Immediately after sacrifice, liver samples were removed and fixed in 10% neutral buffered formalin. Hematoxylin-Eosin staining or Masson's Trichrome staining were performed by the standard manner.

2.4 Statistics

All data were expressed as the mean ± S.E. Data were analyzed for statistical significance with unpaired two-tailed Student's t test. Survival analysis was performed using the Kaplan-Meier method and differences were assessed using the log-rank test with SPSS software

(IBM SPSS statistics 22). P values < 0.05 were considered statistically significant in all analyses.

3. Results

3.1. The technique of the partial common bile duct ligation (pCL) model

The pCL model was originally developed to improve the survival of the standard tCL model [12]. After a median laparotomy incision, the common bile duct is exposed (Fig. 1A). A 7-0 surgical needle is placed by the common bile duct after a 6-0 monofilament suture is passed between the bile duct and portal vein (Fig. 1B). The suture is tied tightly to reproduce the same constriction of lumen size each time (Fig. 1C). The needle is removed leaving a “half-open” bile duct (Fig. 1D).

3.2. Post-operative course after pCL

The standard tCL models have been reported to have high early mortality [3,13] and the pCL model was developed to overcome this shortcoming. Therefore, it was of interest to analyze the postoperative course and complications of the pCL model. Figure 2A demonstrates a representative postoperative course after pCL. The gallbladder (GB) usually begins to expand on postoperative day (POD) 1. The common bile duct begins to dilate and the subcutaneous tissues and liver begin to develop jaundice after POD 3. However, the jaundice improved by POD 14 and compensatory enlargement of the liver is observed.

Three complications that developed 2 days after pCL are demonstrated. They were intraabdominal bleeding (Fig. 2B), liver necrosis (Fig. 2C) and gastric dilation due to intramural hematoma of duodenum (Fig. 2D). All complications occurred during the first 10 cases we performed.

3.3. The technique of the LHML model

For this procedure in particular, we found that exposure of the surgical field is the key for success. We retract the xyphoid superiorly with a cramp and gently hold the middle lobe superiorly for the exposure of murine porta hepatis. The hepatic bile duct is ligated proximal to the point where right hepatic duct branches, and distal to the point where the left and middle hepatic duct merge. The cystic duct is ligated; however, we do not remove the gallbladder to avoid possible operative liver injury (Fig. 3A). When the gallbladder appears enlarged, the bile juice is aspirated with a 27G needle. Regardless of removal of the gallbladder, no cholecystitis is observed after LMHL. No jaundice is observed and the common bile duct is not dilated at POD 1 (Fig. 3B). Common bile duct dilation is observed at POD 18, when the edges of left and middle lobe of the liver are dull and appeared edematous indicating liver injury. On the other hand, the right and caudate lobes are enlarged in a compensatory fashion (Fig. 3C).

3.4. Survival after the obstructive jaundice models

The obstructive jaundice models, tCL, pCL and LMHL, were performed on C57BL/6J mice and their survival was followed (Fig. 4). We found that the LMHL model demonstrated the least mortality with 81% (3/16) survival at Day 14. Some of them even survived over a

month. The pCL model demonstrated 66% (10/15) survival at Day 14. Of note, all the 34% mortality of pCL model occurred within the first 3 days after the procedure and none thereafter, which suggests that there is no life-threatening complication or liver injury occurring after that time. The tCL model demonstrated the worst mortality with 70% (7/10) survival at Day 8.

3.5 Surgical stress/acute inflammation, compensatory liver regeneration, and portal hypertension after pCL and LMHL models

In order to learn the different characteristics of the pCL and LMHL models, physical parameters, such as body weight (BW), liver weight and spleen weight were measured. pCL demonstrated a significant reduction of body weight by POD 3, which recovered by POD 14 compared with Sham controls. No body weight change was observed after LMHL model (Fig. 5A). This suggests that there is more early phase surgical stress or acute inflammation in pCL compared to LMHL. In both models, liver weights were significantly heavier in operated mice by POD 14, which reflects the fact that compensatory liver generation occurs in both models ($p>0.005$ after pCL, $p=0.001$ after LMHL, respectively) (Fig. 5B). The spleen was significantly smaller on Day 3 after pCL ($p=0.001$), which is consistent with acute phase surgical stress and/or acute inflammation. Splenomegaly was observed in LMHL alone, which may reflect portal hypertension 14 days after operation ($p=0.001$) (Fig. 5C).

3.6 pCL model developed acute liver injury, whereas LMHL developed latent liver fibrosis

Based upon the macroscopic findings and physiological parameters, we hypothesized that pCL induces acute liver injury which recovers, whereas LMHL promotes development of long-term cholestasis and liver fibrosis. In order to see whether that is the case, we first measured the serum total bile acid levels (Fig. 6A). We found that the levels after tCL are highly variable which suggests that to obtain stable results using this model is difficult. Total bile acid levels are high on POD 3 after pCL but significantly decrease by POD 7. This indicates that, jaundice decreases in this model over the long term following the operation. On the contrary, total bile acid levels were maintained at high levels in LMHL at POD 7. We found that all the models sustained bile duct injury after surgery, which is clear from ALP levels; whereas there was not much change in AST or ALT. H-E staining revealed more vacuolar degeneration in hepatocyte and bleeding around Glisson's capsule 3 days after pCL, which is consistent with acute liver injury, but not after LMHL (Fig. 6B). Masson-Trichrome staining demonstrated strong fibrotic changes in the liver 14 days after LHML. This finding was absent after pCL (Fig. 6C). Liver RNA expression of collagen 1a1, which is a marker of fibrosis, was significantly higher in Day 14 after LMHL compared from pCL (Fig. 6D).

Discussion

There have been numerous publications regarding bile drainage such as percutaneous transhepatic cholangiodrainage (PTCD), endoscopic nasal bile drainage (ENBD), and biliary stent placement, in obstructive jaundice, which reflects the surgeons' interest in the topic [23–30]. Some do not recommend biliary stent placement for patients undergoing operation

for obstructive jaundice outside of randomized clinical trials [14]. This is partly because the stenting itself may increase the rate of serious adverse events, such as cholangitis. On the other hand, it is well known that obstructive jaundice does cause liver injury and cholangitis, which can hinder operative outcomes and survival or worsen prognosis and quality of life in patients with unresectable tumors [23]. Given this situation, biliary surgeons are forced to balance the advantages and disadvantages of stenting on a case-by-case basis. What is currently missing in the equation is an understanding of the effect of obstructive jaundice on cancer biology and whether elevated conjugated bile acids (CBAs) by obstructive jaundice worsens cancer progression.

In addition to its long recognized function as a detergent, bile acids are now known as important signaling molecules for cells in the liver and gastrointestinal tract [4,15,16] and are involved in the regulation of lipid and glucose metabolism [4–6]. Bile acids can activate several nuclear receptors (FXR-α, PXR, vitamin D receptor (NR12)) and G-protein-coupled receptor (GPCR) membrane-type bile acid receptor (TGR5/M-BAR) [4,5,17]. Additionally, they act on various cell signaling pathways including extracellular regulated kinase (ERK)1/2 and protein kinase B (AKT). Recently, we found that CBAs activate the ERK1/2 and AKT signaling pathways through binding to and activation of S1PR2, another GPCR [5]. In cholangiocarcinoma cells, CBAs enhanced the activation of NF-κB, which was associated with an up-regulation of the expression of IL-6 and COX-2 [18]. We also found that CBAs activate intracellular ERK1/2 and AKT signaling to promote the invasive growth of cholangiocarcinoma via activation of S1PR2 *in vitro* [1,2]. Given these intriguing findings in cell culture systems, appropriate animal models to study the effect of obstructive jaundice are in need.

We investigated the utility of surgical bile duct ligation models: tCL, pCL and LMHL. However, others have established spontaneous bile duct obstruction models such as virus induced murine biliary atresia model and transgenic spontaneous bile stenotic mouse. Viral models are generated by intraperitoneal injection of Rhesus rotavirus into newborn mice, which will develop atresia at the distal end of the common bile duct. Pre-stenotic dilatation are seen in the common bile duct, cystic duct and gallbladder [19]. One of the examples of a transgenic model is the Mdr2 (Abcb4) −/− mouse that spontaneously develops severe biliary fibrosis due to upregulation of profibrogenic and downregulation of fibrolytic genes and activities [20,21]. Since these models do not need operations and jaundice develops spontaneously, it is seen to mimic human patient conditions. On the other hand, because of its spontaneous nature, the degree and time course of obstruction cannot be controlled, resulting in difficulty standardizing the experiments using these models.

We compared the survival between the standard tCL, pCL and newly introduced LMHL models. Classical tCL mice had the shortest survival, and pCL and LMHL with GB removal mice survived longer. It is possible that GB removal may have reduced the frequency of cholecystitis caused by bile duct ligation and this may have improved the survival of LMHL within the gallbladder removal model.

We also analyzed the perioperative complications of the models. Technical errors, such as intraperitoneal bleeding and duodenal hematoma, happened in the first ten cases of the bile

duct ligation procedures. Technical errors could be overcome by honing the skills of the procedure, including adequate lighting and exposure. It has been reported that tCL models generate massive liver damage followed by short survival [3,12]. Based upon our experience, we agree with previous reports that many of causes for short survival of this model may be due to technical inadequacies [22]. In our opinion, tCL is technically the simplest model, however, short survival limits its usage.

We have found that the pCL model develops acute inflammation in the liver by POD 3. This is consistent with body weight loss on POD 3 that recovers by POD 14. The overt jaundice was diminished on POD 14. Given these findings, pCL may be an appropriate model to study acute changes by obstructive jaundice.

On the other hand, the LMHL model develops significant elevation of total bile acid levels together with liver fibrosis seen by Masson-Tricrome staining and collagen expression by POD 14. Further agreement was demonstrated by significantly increased spleen weight, which reflections portal hypertension, in the LMHL model but not the pCL. This is despite the fact that both models develop compensatory liver regeneration by POD 14. Given the simplicity of the LMHL model and our results, fibrosis is most likely due to cholestasis created by bile duct ligation. Development of liver fibrosis by cholestasis in 2 weeks appears rather soon compared to the human. However, considering how quickly murine liver regenerates (7–10 days in mouse vs 1 month in human after 70% hepatectomy), it may be due to the difference in species. Our results suggest that LMHL with cystic duct ligation provides stable jaundice with long-term survival. This may be suitable for studying the effect of obstructive jaundice over a longer period, such as cancer progression. Indeed, fibrosis limits the utility of this model in the cancer development setting with worsened survival. However, we believe that fibrosis is part of the expected result of cholestasis; thus, it may be beneficial that this model includes that aspect as well.

Conclusions

In conclusion, we found that the commonly used total ligation of the common bile duct (tCL) model is too unstable with high mortality for long-term studies. Partial common bile duct ligation (pCL) may be an appropriate model for acute inflammation with obstructive jaundice but jaundice is not sustained in long-term survivors. The ligation of the left and median hepatic bile duct with gallbladder removal (LMHL) was identified to be the most feasible model to study the effect of long-term obstructive jaundice.

Acknowledgments

This work was supported by United States National Institute of Health grants (R01CA160688 to K.T. and R01CA61774 to S.S.) and Susan G. Komen Investigator Initiated Research award IIR12222224 to KT. The authors thank the Department of the Anatomic Pathology Research Services Director, Dr. Jorge A. Almenara, and the histotechnologists for technical assistance with tissue processing, sectioning, and staining. Microscopy was performed in the VCU Department of Anatomy and Neurobiology Microscopy Facility, supported, in part, with funding from the NIH-NINDS Center core grant (5P30NS047463)

Reference

1. Liu R, Li X, Luo L, Qiang X, Hylemon PB, Jiang Z, et al. Taurocholate Induces Cyclooxygenase-2 Expression via the Sphingosine 1-phosphate Receptor 2 in a Human Cholangiocarcinoma Cell Line. J Biol Chem. 2015; 290 jbc.M115.668277.
2. Liu R, Zhao R, Zhou X, Liang X, Campbell DJW, Zhang X, et al. Conjugated bile acids promote cholangiocarcinoma cell invasive growth through activation of sphingosine 1-phosphate receptor 2. Hepatology. 2014:908–918. [PubMed: 24700501]
3. Yang H, Li TWH, Peng J, Tang X, Ko KS, Xia M, et al. A mouse model of cholestasis-associated cholangiocarcinoma and transcription factors involved in progression. Gastroenterology. 2011; 141:378–388. [PubMed: 21440549]
4. Park MA, Zhang G, Norris J, Hylemon PB, Fisher PB, Grant S, et al. Regulation of autophagy by ceramide-CD95-PERK signaling. Autophagy. 2008; 4:929–931. [PubMed: 18719356]
5. Studer E, Zhou X, Zhao R, Wang Y, Takabe K, Nagahashi M, et al. Conjugated bile acids activate the sphingosine-1-phosphate receptor 2 in primary rodent hepatocytes. Hepatology. 2012; 55:267–276. [PubMed: 21932398]
6. Nagahashi M, Takabe K, Liu R, Peng K, Wang X, Wang Y, et al. Conjugated bile acid-activated S1P receptor 2 is a key regulator of sphingosine kinase 2 and hepatic gene expression. Hepatology. 2015; 61:1216–1226. [PubMed: 25363242]
7. Ueno K, Ajiki T, Watanabe H, Abo T, Takeyama Y, Onoyama H, et al. Changes in Extrathymic T Cells in the Liver and Intestinal Intraepithelium in Mice with Obstructive Jaundice. World J Surg. 2004; 28:277–282. [PubMed: 14961202]
8. Miyoshi H, Rust C, Roberts PJ, Burgart LJ, Gores GJ. Hepatocyte apoptosis after bile duct ligation in the mouse involves Fas. Gastroenterology. 1999; 117:669–677. [PubMed: 10464144]
9. Licata, La; Nguyen, CT.; Burga, Ra; Falanga, V.; Espat, NJ.; Ayala, A., et al. Biliary obstruction results in PD-1-dependent liver T cell dysfunction and acute inflammation mediated by Th17 cells and neutrophils. J Leukoc Biol. 2013; 94:1–11. [PubMed: 23818015]
10. Tiao M-M, Wang F-S, Huang L-T, Chuang J-H, Kuo H-C, Yang Y-L, et al. MicroRNA-29a protects against acute liver injury in a mouse model of obstructive jaundice via inhibition of the extrinsic apoptosis pathway. Apoptosis. 2014; 19:30–41. [PubMed: 24052410]
11. Tag CG, Sauer-Lehnen S, Weiskirchen S, Borkham-Kamphorst E, Tolba RH, Tacke F, et al. Bile Duct Ligation in Mice: Induction of Inflammatory Liver Injury and Fibrosis by Obstructive Cholestasis. J Vis Exp. 2015:1–11.
12. Heinrich S, Georgiev P, Weber A, Vergopoulos A, Graf R, Clavien PA. Partial bile duct ligation in mice: A novel model of acute cholestasis. Surgery. 2011; 149:445–451. [PubMed: 20817234]
13. Kirkland JG, Godfrey CB, Garrett R, Kakar S, Yeh BM, Corvera CU. Reversible surgical model of biliary inflammation and obstructive jaundice in mice. J Surg Res. 2010; 164:221–227. [PubMed: 19932898]
14. Fang Y, Wang Q, Ks G, Lin H, Xie X, Wang C. Preoperative biliary drainage for obstructive jaundice (Review). Cochrane Database Syst Rev. 2012
15. Xu Z, Tavares-Sanchez OL, Li Q, Fernando J, Rodriguez CM, Studer EJ, et al. Activation of Bile Acid Biosynthesis by the p38 Mitogen-activated Protein Kinase (MAPK): HEPATOCYTE NUCLEAR FACTOR-4 PHOSPHORYLATION BY THE p38 MAPK IS REQUIRED FOR CHOLESTEROL 7 -HYDROXYLASE EXPRESSION. J Biol Chem. 2007; 282:24607–24614. [PubMed: 17603092]
16. Zhang G, Park M, Mitchell C, Walker T, Hamed H, Studer E, et al. Multiple Cyclin Kinase Inhibitors Promote Bile Acid-induced Apoptosis and Autophagy in Primary Hepatocytes via p53-CD95-dependent Signaling. 2008 [accessed January 20, 2016] http://www.jbc.org/content/283/36/24343.full.pdf.
17. Hylemon PB, Zhou H, Pandak WM, Ren S, Gil G, Dent P. Bile acids as regulatory molecules. J Lipid Res. 2009; 50:1509–1520. [accessed January 20, 2016] http://www.jlr.org/content/50/8/1509.full.pdf. [PubMed: 19346331]
18. Dai J, Wang H, Shi Y, Dong Y, Zhang Y, Wang J. Impact of bile acids on the growth of human cholangiocarcinoma via FXR. J Hematol Oncol. 2011; 4:41. [PubMed: 21988803]

19. Petersen C, Grasshoff S, Luciano L. Diverse morphology of biliary atresia in an animal model. J Hepatol. 1998; 28(4):603–607. [PubMed: 9566828]
20. Popov Y, Patsenker E, Fickert P, Trauner M, Schuppan D. Mdr2 (Abcb4)−/− mice spontaneously develop severe biliary fibrosis via massive dysregulation of pro- and antifibrogenic genes. J Hepatol. 2005; 43:1045–1054. [PubMed: 16223543]
21. Smit JJ, Schinkel aH, Oude Elferink RP, Groen aK, Wagenaar E, van Deemter L, et al. Homozygous disruption of the murine mdr2 P-glycoprotein gene leads to a complete absence of phospholipid from bile and to liver disease. Cell. 1993; 75:451–462. [PubMed: 8106172]
22. Tag C, Weiskirchen S, Hittatiya K, Tacke F, Tolba R, Weiskirchen R. Induction of experimental obstructive cholestasis in mice. Lab Anim. 2015; 49:70–80. [PubMed: 25835740]
23. Wu J, Song L, Zhang Y, Zhao DY, Guo B, Liu J. Efficacy of percutaneous transhepatic cholangiodrainage (PTCD) in patients with unresectable pancreatic cancer. Tumour Biol. 2014 Mar; 35(3):2753–2757. [PubMed: 24264311]
24. Kloek JJ, van der Gaag NA, Aziz Y, Rauws EA, van Delden OM, Lameris JS, Busch OR, Gouma DJ, van Gulik TM. Endoscopic and percutaneous preoperative biliary drainage in patients with suspected hilar cholangiocarcinoma. J Gastrointest Surg. 2010 Jan; 14(1):119–125. [PubMed: 19756881]
25. Kawakami H, Kuwatani M, Onodera M, Haba S, Eto K, Ehira N, Yamato H, Kudo T, Tanaka E, Hirano S, Kondo S, Asaka M. Endoscopic nasobiliary drainage is the most suitable preoperative biliary drainage method in the management of patients with hilar cholangiocarcinoma. J Gastroenterol. 2011 Feb; 46(2):242–248. [PubMed: 20700608]
26. Kawashima H, Itoh A, Ohno E, Itoh Y, Ebata T, Nagino M, Goto H, Hirooka Y. Preoperative endoscopic nasobiliary drainage in 164 consecutive patients with suspected perihilar cholangiocarcinoma: a retrospective study of efficacy and risk factors related to complications. Ann Surg. 2013 Jan; 257(1):121–127. [PubMed: 22895398]
27. Iacono C, Ruzzenente A, Campagnaro T, Bortolasi L, Valdegamberi A, Guglielmi A. Role of preoperative biliary drainage in jaundiced patients who are candidates for pancreatoduodenectomy or hepatic resection: highlights and drawbacks. Ann Surg. 2013 Feb; 257(2):191–204. [PubMed: 23013805]
28. Nagino M, Takada T, Miyazaki M, Miyakawa S, Tsukada K, Kondo S, Furuse J, Saito H, Tsuyuguchi T, Yoshikawa T, Ohta T, Kimura F, Ohta T, Yoshitomi H, Nozawa S, Yoshida M, Wada K, Amano H, Miura F. Japanese Association of Biliary Surgery; Japanese Society of Hepato-Biliary-Pancreatic Surgery; Japan Society of Clinical Oncology. Preoperative biliary drainage for biliary tract and ampullary carcinomas. J Hepatobiliary Pancreat Surg. 2008; 15(1):25–30. [PubMed: 18274841]
29. Nimura Y, Kamiya J, Kondo S, Nagino M, Uesaka K, Oda K, Sano T, Yamamoto H, Hayakawa N. Aggressive preoperative management and extended surgery for hilar cholangiocarcinoma: Nagoya experience. J Hepatobiliary Pancreat Surg. 2000; 7(2):155–162. [PubMed: 10982608]
30. Kloek JJ, van der Gaag NA, Aziz Y, Rauws EA, van Delden OM, Lameris JS, Busch OR, Gouma DJ, van Gulik TM. Endoscopic and percutaneous preoperative biliary drainage in patients with suspected hilar cholangiocarcinoma. J Gastrointest Surg. 2010 Jan; 14(1):119–125. [PubMed: 19756881]

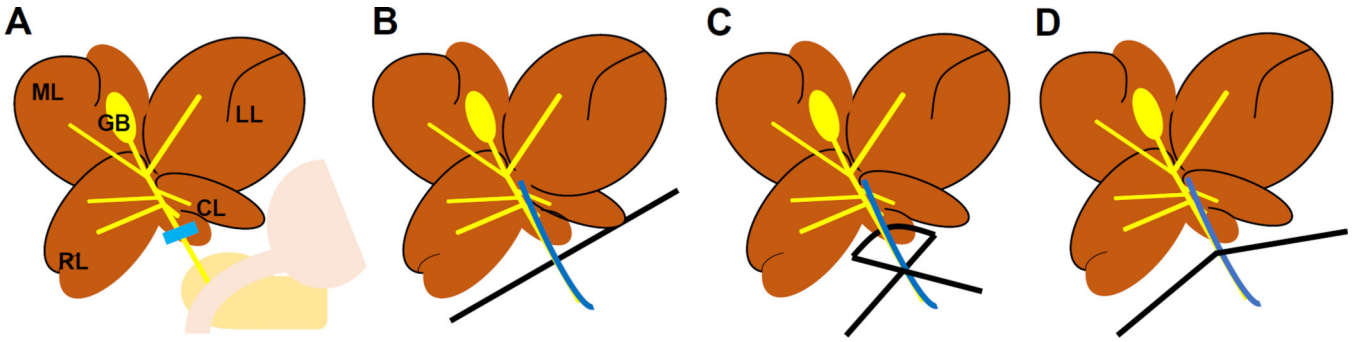

Figure 1. The procedure of partial common duct ligation (pCL) model

A median laparotomy incision was made and the common bile duct is exposed. (A) After a 6-0 monofilament suture is placed around the bile duct and a 7-0 surgical needle (B), the suture is tied tightly (C). The needle is removed leaving a defined lumen with the ligation of the bile duct (D). Abbreviations used; ML, median lobe; LL, left lobe; CL, caudate lobe; RL, right lobe; GB, gallbladder.

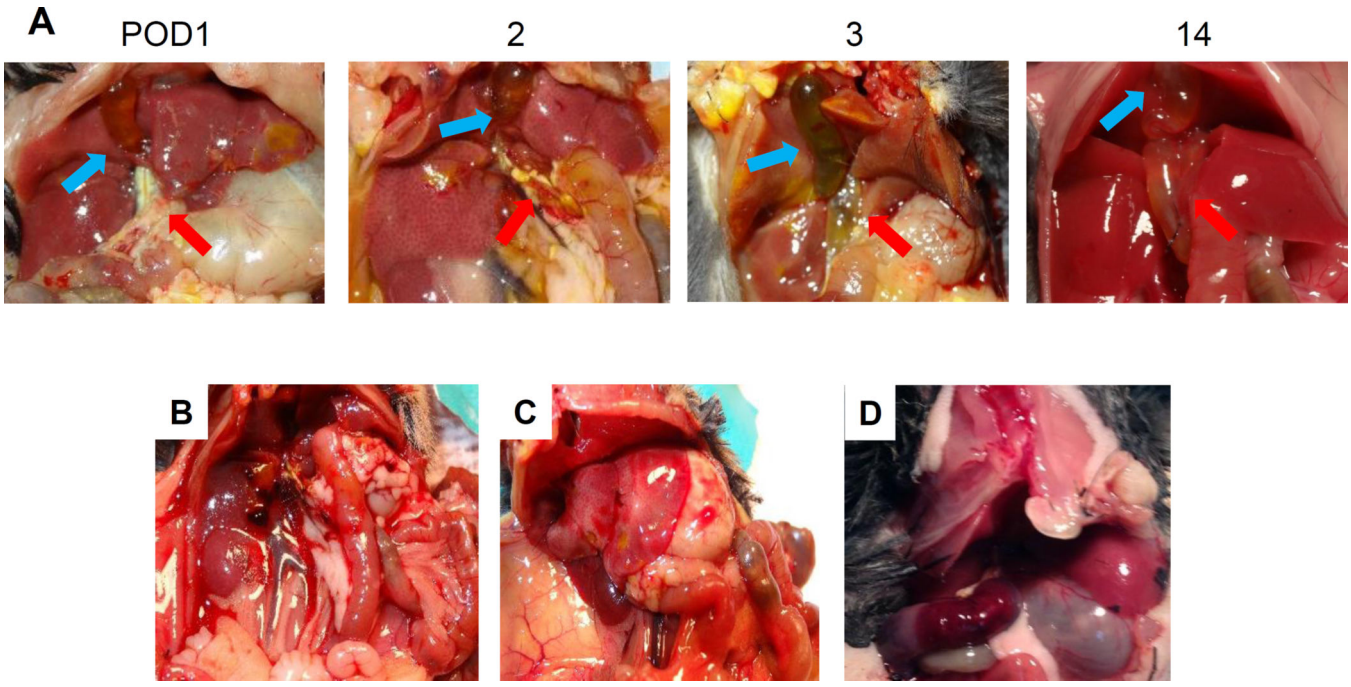

Figure 2. Postoperative course of pCL model

(A) Representative postoperative course after pCL, demonstrating POD 1, 2, 3, and 14. Jaundice is observed on POD 3 but decreased and compensatory enlargement of liver is observed on POD 14. Complications were (B) Intraperitoneal bleeding, (C) Liver failure, and (D) Duodenum hematoma with gastric distention.

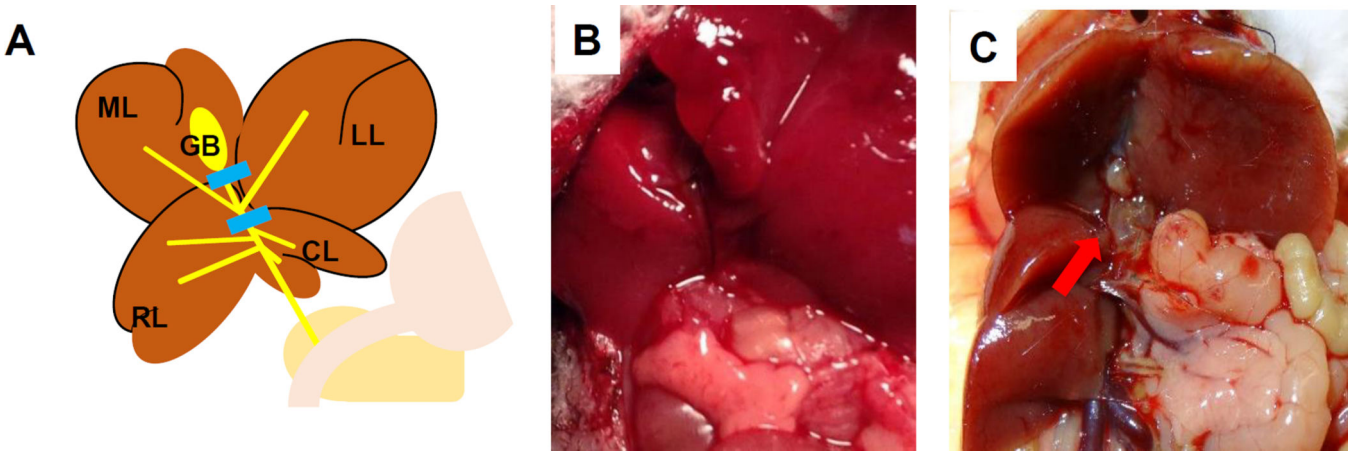

Figure 3. The procedure of left and median hepatic bile duct ligation with gallbladder removal (LMHL) model

(A) The hepatic bile duct is ligated distal to the merging point of the left and median hepatic bile duct and proximal to the union of the right and caudate hepatic bile duct. (B) Representative image that common bile duct is not dilated and liver appeared normal on POD 1. (C) The edges of the left and middle lobes of the liver are dull and lobes are edematous and yellowish. Right and caudate lobes are hypertrophic on Day 18. Dilated hepatic bile duct is indicted with red arrow.

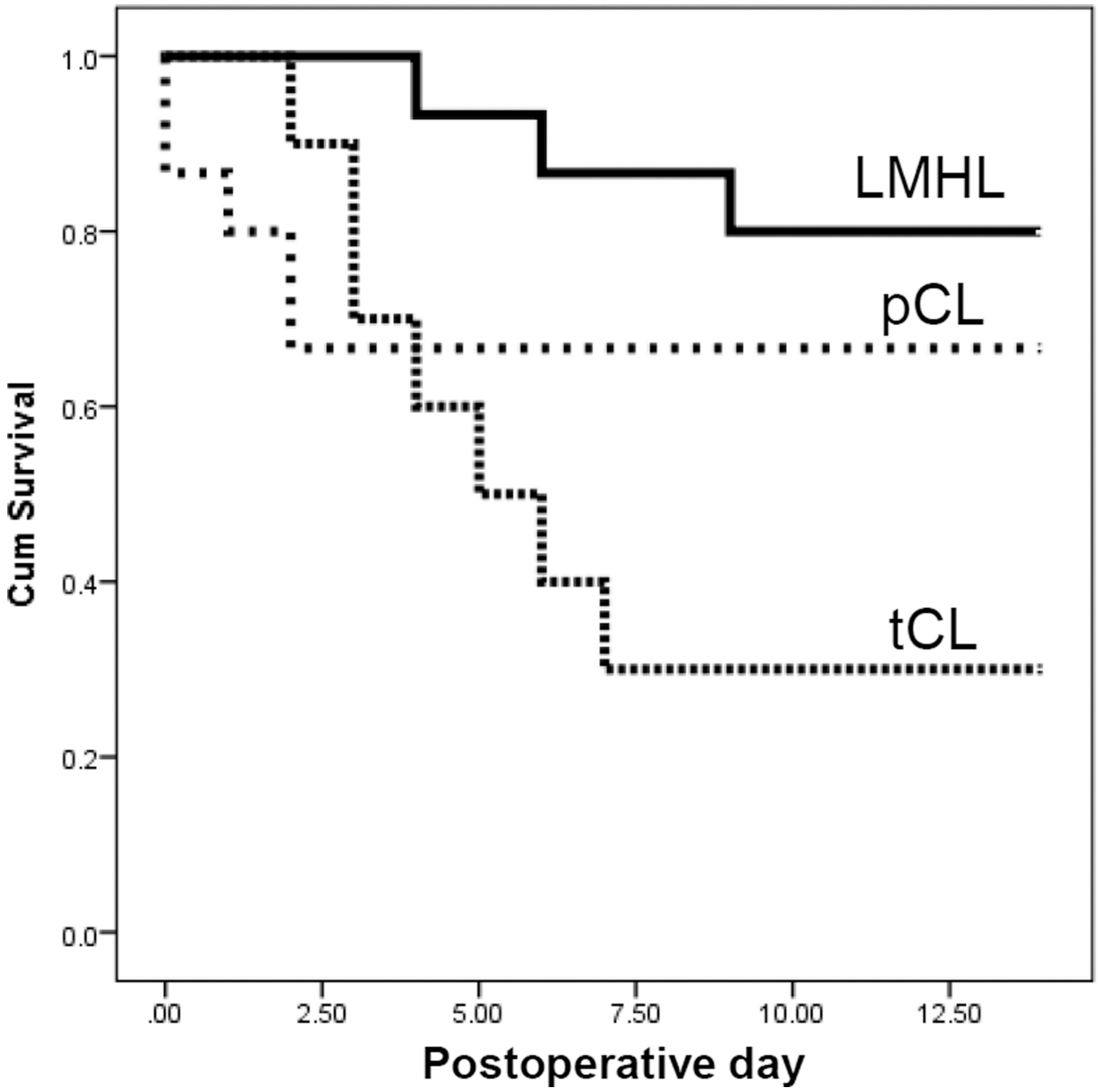

Figure 4. Survival of mice after tCL, pCL or LMHL operations

Fine dotted line indicates after tCL, coarse line indicates after pCL, and bold line indicates survival after LHML model coarse dotted line indicates pCL model, and fine dotted line indicate tCL, respectively.

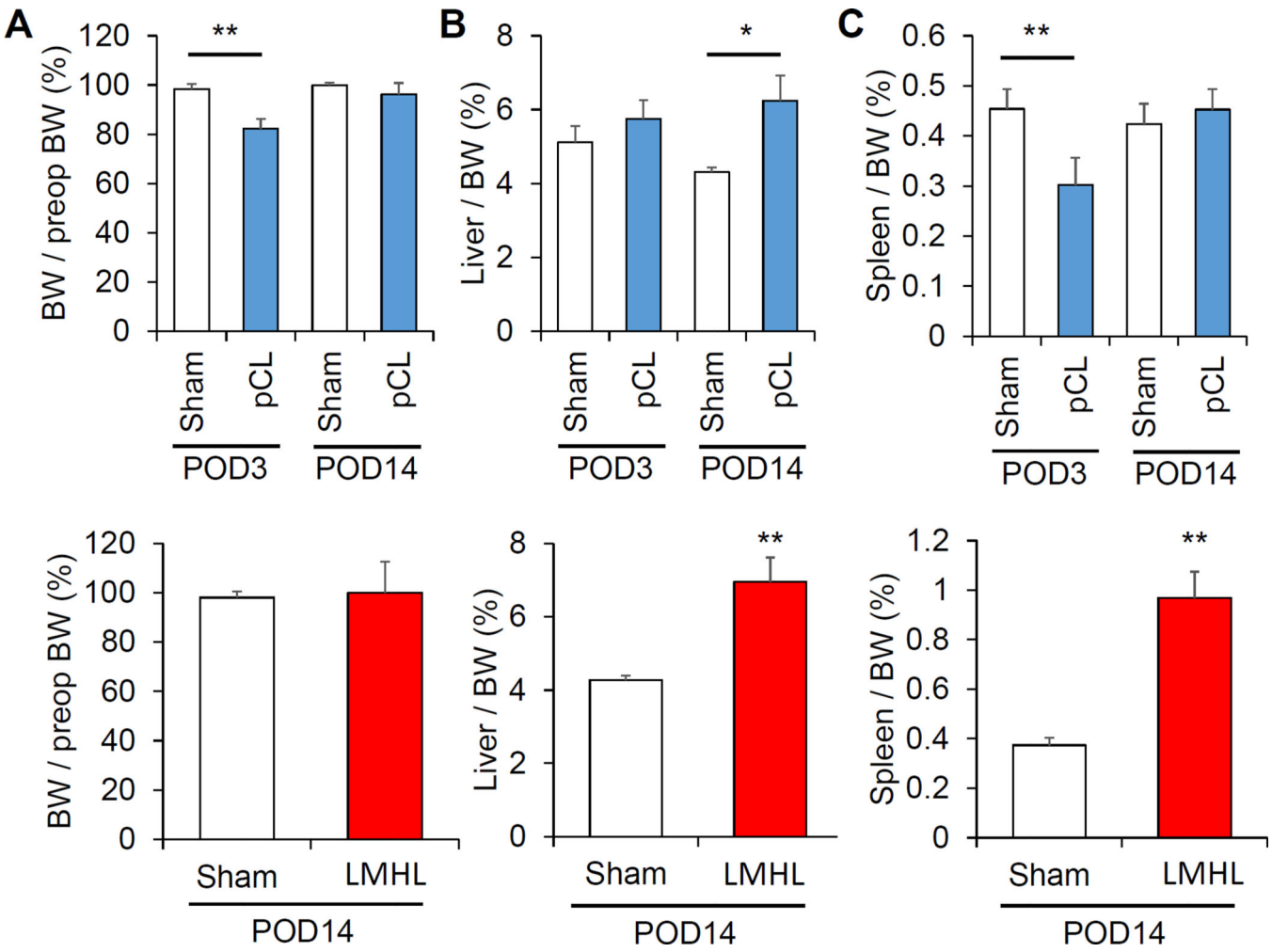

Figure 5. Surgical stress/acute inflammation, compensatory liver regeneration, and portal hypertension after pCL and LMHL models

(A) pCL model (blue column) showed significant reduction of body weight (BW) on POD3 that recovered on POD14 compared from Sham (white column), whereas no change in BW was seen after LMHL (red column). (B) Liver weight per BW were increased in both groups at POD14. (C) Spleen is significantly smaller on Day 3 after pCL model. Splenomegaly was observed in LMHL model. Data are expressed as mean±SEM, *, P<0.05,**, p<0.001, compared with the control Sham group.

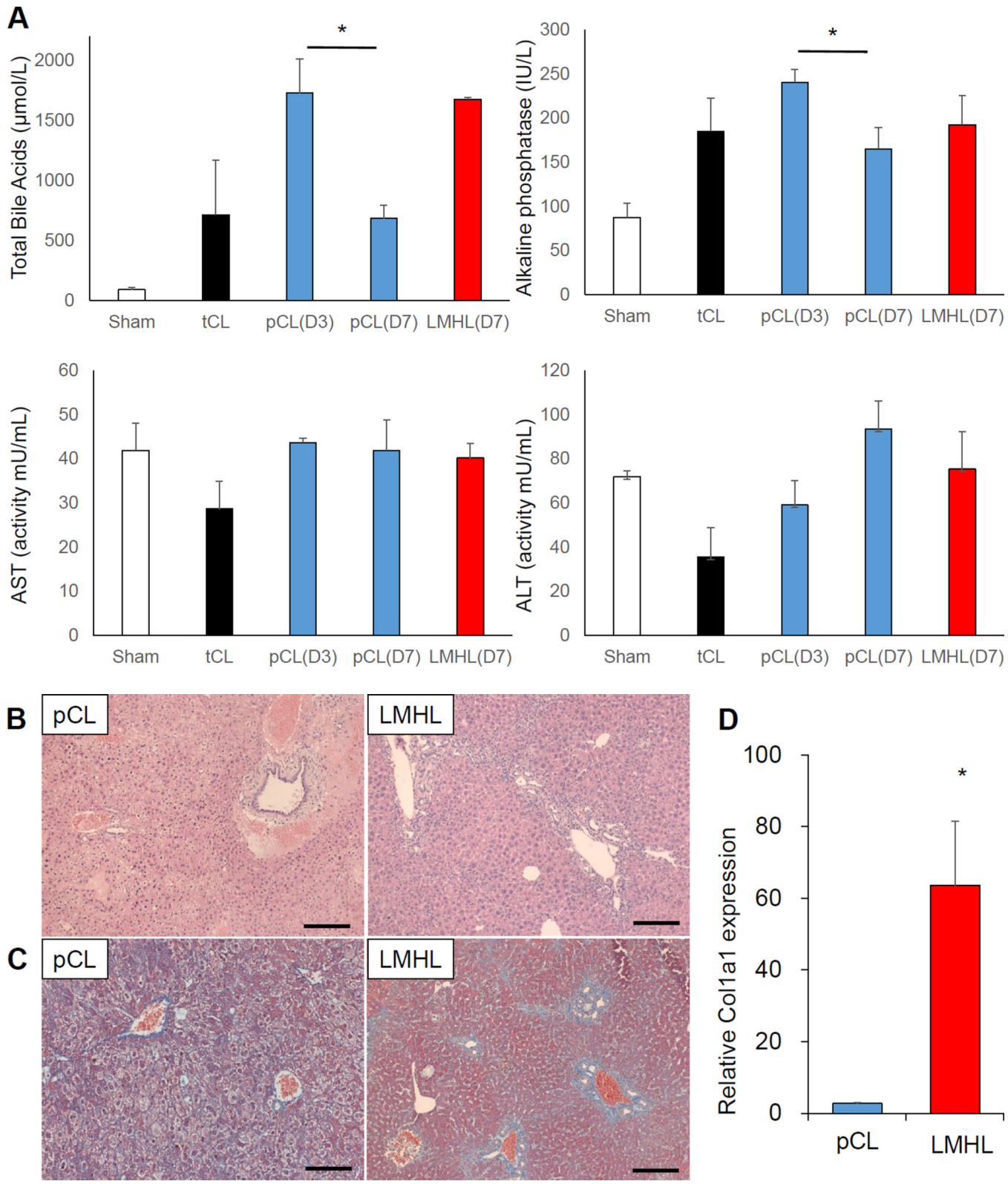

Figure 6. pCL model developed acute liver injury, whereas LMHL developed latent liver fibrosis

(A) Serum total bile acids, alkaline phosphatase (ALP), AST and ALT are measured 3 days after Sham (white column), tCL (black column), and pCL(D3) (blue column), and 7 days after pCL(D7) (blue column) and LMHL(D7) (red column). (B) H-E staining showed the acute inflammation with less fibrotic change in pCL model at POD3. (C) In LMHL model significant fibrosis was observed on POD 14 by Masson-Trichrom staining. Scale bar, 200 μm. (D) collagen1a1 expression were significantly higher in the liver of LMHL POD 14 compared from pCL. Data are expressed as mean±SEM, *, $P<0.05$,**.